Benzodithiophene–Thiadiazoloquinoxaline as an Acceptor for Ambipolar Copolymers with Deep LUMO Level and Distinct Linkage Pattern

ARTICLE *in* MACROMOLECULES · JANUARY 2014

Impact Factor: 5.8 · DOI: 10.1021/ma401938m

Macromolecules

Article

pubs.acs.org/Macromolecules

Benzodithiophene−Thiadiazoloquinoxaline as an Acceptor for Ambipolar Copolymers with Deep LUMO Level and Distinct Linkage Pattern

Cunbin An, Sreenivasa Reddy Puniredd,† Xin Guo, Timea Stelzig,‡ Yanfei Zhao, Wojciech Pisula, and Martin Baumgarten*

Max Planck Institute for Polymer Research, Ackermannweg 10, 55128 Mainz, Germany

Supporting Information

ABSTRACT: Two new conjugated copolymers, **PBDTTQ-1** and **PBDTTQ-2**, with a distinct linked pattern between benzodithiophene−thiadiazoloquinoxaline (**BDTTQ**) as acceptor and bithiophene as donor were synthesized and characterized. The difference in the linkage between donor and acceptor exerts great influence on the optoelectronic properties of the two polymers. The optical band gap decreases from 1.18 eV for **PBDTTQ-1** to 1.03 eV for **PBDTTQ-2**, due to the lower LUMO energy level (−4.01 eV) of the latter. Moreover, density functional theory calculations demonstrate that the electron density is mainly confined on the acceptor unit in both HOMO and LUMO of **PBDTTQ-1**, while the electronic densities almost delocalize along the entire backbone of **PBDTTQ-2**, which facilitates the charge transport within the polymer chain. In contrast to **PBDTTQ-1** missing any field-effect characteristics, **PBDTTQ-2** exhibits ambipolar charge transporting behavior with mobilities of 1.2×10^{-3} $cm^2/(V\ s)$ for holes and 6.0×10^{-4} $cm^2/(V\ s)$ for electrons.

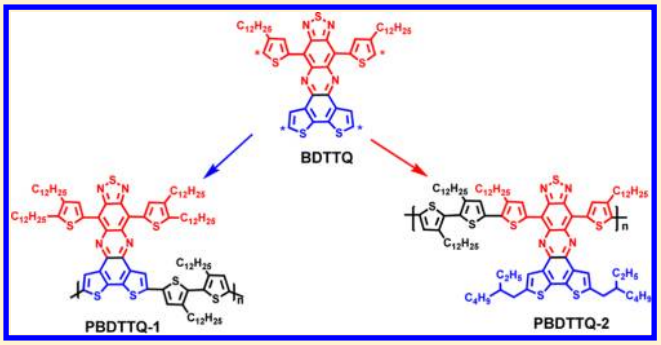

INTRODUCTION

Low bandgap π-conjugated copolymers composed of alternating donor (D) and acceptor (A) moieties have proven to be successful in improving device properties in organic light-emitting diodes (OLEDs), polymer solar cells (PSCs) and organic field-effect transistors (OFETs).[1−5] The strong acceptor can be beneficial for developing low bandgap copolymers with deep LUMO levels, which imparts characteristics of transporting negative charge through the polymers and improves the stability. Currently, some strong acceptors have been applied to make promising D−A copolymers, such as benzobisthiadiazole (BBT),[6,7] naphthalene diimide (NDI),[8,9] diketopyrrolopyrrole (DPP),[10,11] and perylene diimide (PDI).[12,13] The development of new strong acceptors that can be used for constructing D−A polymers with deep LUMO level and ambipolar charge carrier transport remains still challenging.

Thiadiazoloquinoxalines (TQs) are much stronger electron acceptors (LUMO∼ −3.43 to −3.83 eV)[14,15] than DPP (provide LUMO∼ −3.13 eV),[16] as previously indicated by redox potential, and can be modified in order to increase the solubility or improve device performance via functionalization at the 6 and 7 positions (Figure 1, I).[17−21] Copolymers made from TQs have been reported as promising p-type semiconductors. In these polymers, TQs which were usually flanked with two thiophene units at the 4 and 9 positions were copolymerized with donors such as fluorene,[22] thiophene[23] and dithieno[3,2-*b*:2′,3′-*d*]pyrrole[24] and only a few copolymers showed decent hole transporting properties, but no ambipolar behavior was observed. Introducing acetylenic π-spacers into the main chains of TQ-based polymers can reduce the twist within the polymer backbones (Figure 1, II),[15] leading to ambipolar polymer semiconductors.[25] The extension of π-conjugation length in the TQ core has also been proven to effectively lower the LUMO level and strengthen the electron-withdrawing ability.[26] However, these extended fused TQs derivatives have not been used as acceptors to construct D−A copolymers applied in OFETs until now.

Benzodithiophene-thiadiazoloquinoxaline (**BDTTQ**) was thus designed by fusing the thiophene rings to form a larger π-conjugated system (Figure 1, III). This new acceptor can be expected to provide lower LUMO level and electron transporting property when being incorporated into the polymer backbone. More interestingly, the **BDTTQ** unit possesses two couples of active positions (a and b in Figure 1, III) for polymerization, which offers an opportunity to make D−A polymers with distinct linked pattern between **BDTTQ** core and donors. In view of the different density electron distribution on the **BDTTQ** core (electron-donating BDT part and electron-accepting TQ part), we can tune the optical

Received: September 18, 2013
Revised: January 3, 2014

   dx.doi.org/10.1021/ma401938m | *Macromolecules* XXXX, XXX, XXX−XXX

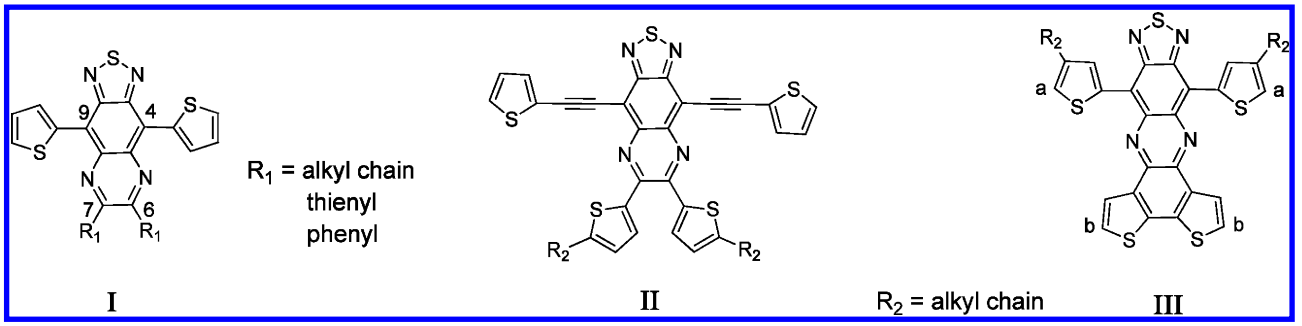

Figure 1. TQ-based acceptors from the literature[21−24] and a new TQ acceptor III presented in this work.

behavior, energy levels, as well as the transport behavior of the copolymers by changing the linking pathway.

In this paper, we report two new D−A copolymers (**PBDTTQ-1** and **PBDTTQ-2**, Scheme 1) containing **BDTTQ** (Figure 1, III) as acceptor. To increase the solubility of both copolymers, substituents as n-dodecyl and 2-ethylhexyl were introduced for **PBDTTQ-1** and **PBDTTQ-2**, respectively. In spite of having same donor and acceptor units in the polymers, both polymers present remarkably different electron distributions and D−A interactions in the polymer chains. For **PBDTTQ-1**, the **BDT** part of **BDTTQ** is located in the conjugated backbone, whereas the **TQ** moiety is suspended around the periphery of the polymer main chains, which is believed that the electron density will be mostly confined on the **TQ** moiety, thereby weakening the charge transfer between donor and acceptor units. In comparison, the **TQ** moiety of **BDTTQ** in **PBDTTQ-2** fully participates in the conjugation along the polymer main chain facilitating the D−A interaction. Comparative investigations on both polymers revealed that the linked pattern in **PBDTTQ-2** is far better extension of conjugation thereby lowering the bandgap, deepening the LUMO level, and improving the charge carrier transport. As a result, **PBDTTQ-2** could be used as an ambipolar semiconducting material in OFET, while **PBDTTQ-1** did not exhibit noticeable field-effect response.

EXPERIMENTAL SECTION

General Methods. ^{1}H NMR and ^{13}C NMR spectra were recorded in deuterated solvents on a Bruker DPX 250. High resolution mass spectra (HRMS) were carried out by the Microanalytical Laboratory of Johannes Gutenberg University, Mainz. UV−Vis-NIR absorption spectra were measured on a Perkin-Elmer Lambda 9 spectrophotometer at room temperature. Thermogravimetry analysis (TGA) were carried out on a Mettler 500 Thermogravimetry Analyzer. Differential scanning calorimetry (DSC) were measured on a Mettler DSC 30 with heating and cooling rates of 10 K/min. Cyclic Volatammetry (CV) were carried out on a computer-controlled GSTAT12 in a three-electrode cell in anhydrous acetonitrile solution of Bu_4NPF_6 (0.1 M) with a scan rate of 50 mV/s at room temperature under argon. A Pt wire, a silver wire, and a glassy carbon electrode were used as the counter electrode, the reference electrode, and the working electrode, respectively. The molecular weights were determined by PSS-WinGPC (PSS) (pump: alliance GPC 2000) GPC equipped with an UV or RI detector running in tetrahydrofuran at 30 °C using a PLgel MIXED-B column (particle size, 10 mm; dimension, 0.8 × 30 cm) calibrated against polystyrene standards. Density functional theory (DFT) calculations were performed using the Gaussian 03 program[27] with the B3LYP hybrid functional[28,29] and basis set 6-31G(d) for the ground state geometry optimization.

OFET Device Fabrication and Measurements. All FETs were fabricated employing the bottom-gate, bottom-contact architecture. The 200 nm thick SiO_2 dielectric covering the highly doped Si acting as the gate electrode was functionalized with hexamethyldisilazane (HMDS) to minimize interfacial trapping sites. Polymer thin films were deposited by spin-coating 10 mg mL^{-1} $CHCl_3$ solution (1200 rpm for 60 s) on FET substrates in nitrogen atmosphere, followed by annealing at 150 °C for 1 h. The channel lengths and widths are 20 and 1400 μm, respectively. All the electrical measurements (using Keithley 4200 SCS) were performed in a glovebox under nitrogen atmosphere.

Two-Dimensional Wide-Angle X-ray Scattering (2D-WAXS). 2D-WAXS measurements were performed using a custom setup consisting of the Siemens Kristalloflex X-ray source (copper anode X-ray tube, operated at 35 kV/20 mA), Osmic confocal MaxFlux optics, two collimating pinholes (1.0 and 0.5 mm Owis, Germany) and an antiscattering pinhole (0.7 mm − Owis, Germany). The patterns were recorded on a MAR345 image plate detector (Marresearch, Germany). The samples were prepared by filament extrusion using a home-built mini-extruder.

Grazing Incidence Wide-Angle X-ray Scattering (GI-WAXS). GIWAXS measurements were performed using a custom setup consisting of rotating anode X-ray source (Rigaku Micromax). By orienting the substrate surface at or just below the critical angle for total reflection with respect to the incoming X-ray beam (~0.2°), scattering from the deposited film was maximized with respect to scattering from the substrate. The GIWAXS data were acquired using a camera comprising an evacuated sample chamber with an X-ray photosensitive image plate. A rotating Cu anode operating at 42 kV and 20 mA (Cu Kα, λ = 1.5418 Å) was used as X-ray source, focused, and monochromatized by a 1D multilayer. Diffraction patterns were recorded on a MAR345 image plate detector.

Synthetic Details. All chemicals and reagents were used as received from commercial sources without further purification unless stated otherwise. Chemical reactions were carried out under ambient atmosphere. Intermediates 2-bromo-3-dodecylthiophene (**1**),[30] 4,7-dibromo-5,6-dinitro-2,1,3-benzothiadiazole (**4**),[31] 2,5-dibromo- benzo-[2,1-*b*:3,4-*b*′]dithiophene-7,8-quinone (**7**),[32] 2-trimethyl-4-dodecylthiophene (**11**),[33] and 5,5′-bis(trimethylstannyl)-3,3′-didodecyl-2,2′-bithiophene (**15**)[34] were prepared according to the literature procedures.

2,3-Didodecylthiophene (2). 2-Bromo-3-dodecylthiophene (**1**) (2.5 g, 7.54 mmol) and Ni(dppp)Cl_2 (48.78 mg, 0.09 mmol) were dissolved in dry diethyl ether (20 mL) in a 100 mL flask. The mixture was cooled down to 0 °C, and n-dodecylmagnesium bromide (9.05 mL, 9.05 mmol, 1 M in diethyl ether) was added dropwise within 10 min. The resulting mixture was refluxed for 4 days, cooled down to room temperature, poured into 100 mL of ice water and hydrolyzed with 1 N HCl. The mixture was extracted with diethyl ether (3 × 20 mL). The combined organic phases were dried with Mg_2SO_4, and the solvent was removed under reduced pressure to afford a dark-red oil, which was purified by reduced pressure distillation (0.75 mbar; 180 °C) to give 2.49 g (colorless oil, 79%) of compound **2**. ^{1}H NMR (250 MHz, CD_2Cl_2): δ 7.01 (d, J = 5.00 Hz 1H), 6.80 (d, J = 5.25 Hz 1H), 2.71 (t, J = 7.50 Hz, 2H), 2.50 (t, J = 7.25 Hz, 2H), 1.64−1.52 (m, 4H), 1.27 (br, 36H), 0.88 (m, 6H). ^{13}C NMR (62.5 MHz, CD_2Cl_2): δ 139.28, 138.31, 129.13, 121.24, 32.53, 32.42, 31.39, 30.17, 30.14, 30.12, 30.08, 30.00, 29.98, 29.90, 29.85, 28.61, 28.17, 23.18, 14.35.

dx.doi.org/10.1021/ma401938m | Macromolecules XXXX, XXX, XXX−XXX

Scheme 1. Synthetic Routes for Two BDTTQ Monomers and Two BDTTQ-Based Polymers.[a]

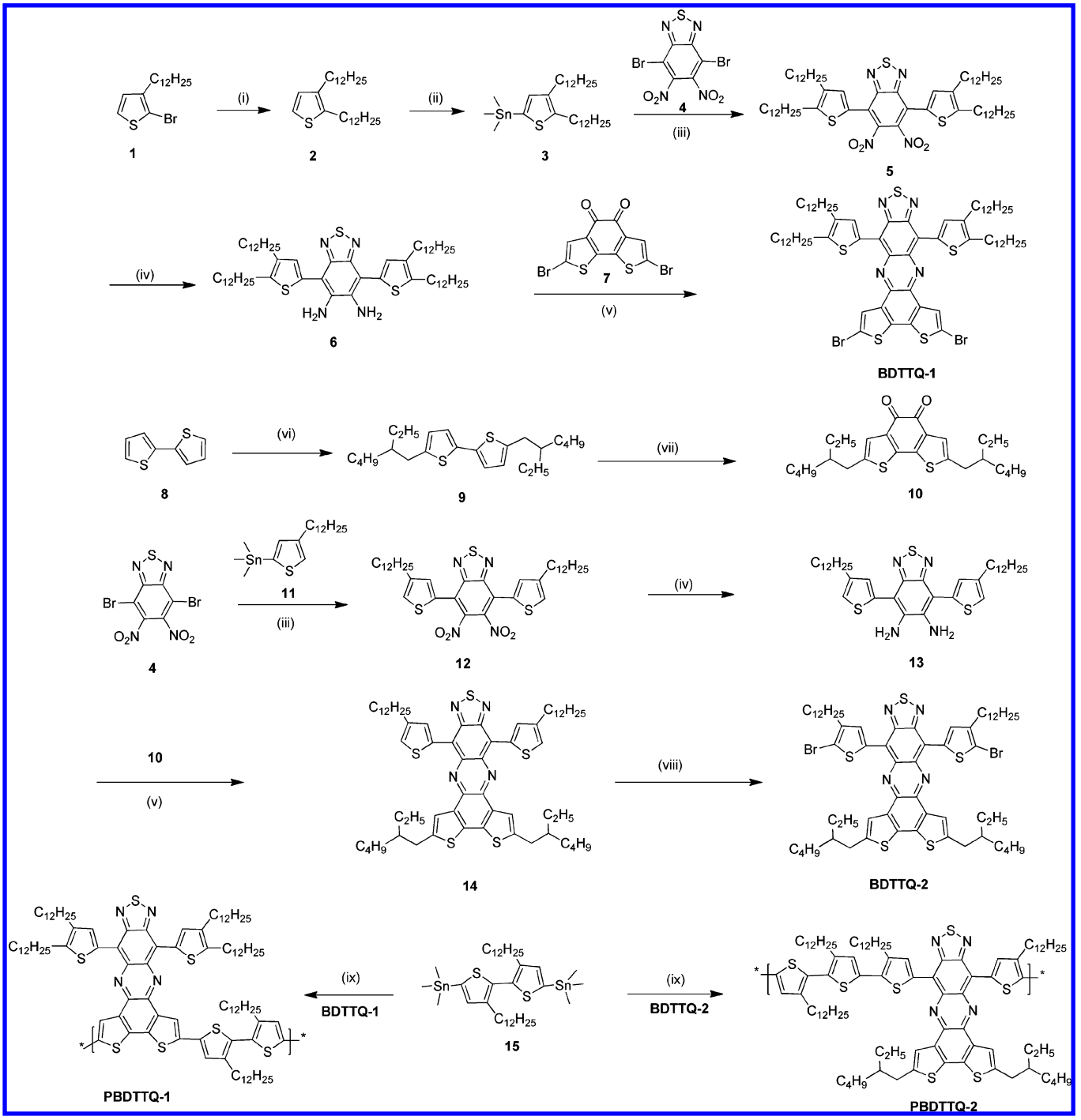

[a]Reagents and conditions: (i) $C_{12}H_{25}MgBr$, Et_2O, $Ni(dppp)Cl_2$, 50 °C, 4 days, 79%; (ii) *n*-BuLi, THF, 0 °C, $(CH_3)_3SnCl$, room temperature, overnight, 80%; (iii) $Pd(PPh_3)Cl_2$, THF, 80 °C, 16 h, 51% for compound **5**, 88% for compound **12**; (iv) Fe, CH_3COOH, 75 °C, 5 h, 85% for compound **6**, 82% for compound **13**; (v) CH_3COOH, 55 °C, overnight, 55% for **BDTTQ-1**, 73% for compound **14**; (vi) *n*-BuLi, *t*-BuOK, THF, −78 °C, ethylhexyl bromide, 70 °C, 12 h, 43%; (vii) 1,2-dichloroethane, pyridine, oxalyl chloride $AlCl_3$, −10 °C to room temperature, 5 h, 47%; (viii) NBS, room temperature, 5 h, 78%; (ix) chlorobenzene, $Pd_2(dba)_3$, tri(*o*-tolyl)phosphine, 110 °C, 3 days, 59% for **PBDTTQ-1**, 63% for **PBDTTQ-2**.

2-Trimethylstannyl-4,5-didodecylthiophene (3). 2,3-Didodecylthiophene (**2**) (1.80 g, 4.28 mmol) was dissolved in 36 mL of anhydrous THF. The mixture was cooled down to 0 °C, and *n*-BuLi (4.0 mL, 6.40 mmol, 1.6 M in hexane) was added slowly whithin 15 min. The resulting solution was stirred for 20 min at 0 °C and warmed to room temperature over 30 min. The mixture was cooled down to 0 °C again, and trimethyltin chloride (6.40 mL, 6.40 mmol, 1 M in hexane) was added dropwise. The mixture was stirred overnight, then poured into water and extracted with ether. The combined organic phases were washed with brine, dried by $MgSO_4$, and filtered. The filtrate was concentrated under reduced pressure to obtain compound **3** (yellow oil, 80%). This crude product was used for next step without further purification. ^1H NMR (250 MHz, CD_2Cl_2): δ 6.89 (s, 1H), 2.72 (t, J = 7.75 Hz, 2H), 2.50 (t, J = 7.50 Hz, 2H), 1.66−1.52 (m,

dx.doi.org/10.1021/ma401938m | *Macromolecules* XXXX, XXX, XXX−XXX

4H), 1.27 (br, 36H), 0.88 (m, 6H), 0.31 (m, 9H). ^{13}C NMR (62.5 MHz, CD_2Cl_2): δ 145.22, 139.77, 137.72, 132.73, 32.57, 32.42, 31.58, 30.17, 30.14, 30.11, 29.85, 28.59, 28.39, 23.17, 14.35, −8.27.

4,7-Bis(4,5-didodecylthiophen-2-yl)-5,6-dinitrobenzo[*c*]-[1,2,5]thiadiazole (5). 4,7-Dibromo-5,6-dinitrobenzodiazole (**4**) (441.6 mg, 1.15 mmol), compound **3** (1.88 g, 3.22 mmol), and $Pd(PPh_3)Cl_2$ (81.4 mg, 0.12 mmol) were dissolved in 25 mL of anhydrous THF under argon. The resulting solution was stirred for 16 h at 80 °C. The solvent was removed under reduced pressure to afford a dark-red oil, which was purified by column chromatography to give 0.62 g (deep red solid, 51%) of compound **5**. ^{1}H NMR (250 MHz, CD_2Cl_2): δ 7.25 (s, 2H), 2.83 (t, J = 7.50 Hz, 4H), 2.57 (t, J = 7.50 Hz, 4H), 1.73−1.68 (m, 4H), 1.58−1.52 (m, 4H), 1.27 (br, 72H), 0.90−0.85 (m, 12H). ^{13}C NMR (62.5 MHz, CD_2Cl_2): δ 152.67, 147.43, 141.61, 140.04, 133.40, 125.65, 121.35, 32.39, 32.11, 31.09, 30.15, 30.11, 30.07, 30.00, 29.93, 29.88, 29.82, 28.60, 28.49, 23.15, 14.32. HRMS (ESI + Na): m/z calcd, 1085.6961; found, 1085.6970.

4,7-Bis(4,5-didodecylthiophen-2-yl)benzo[*c*][1,2,5]-thiadiazole-5,6-diamine (6). Compound **5** (0.3 g, 0.28 mmol) and fine iron powder (186 mg, 3.32 mmol) in acetic acid (8 mL) was stirred for 5 h at 75 °C. The reaction mixture was cooled down to room temperature, precipitated in 5% aqueous NaOH and extracted with diethyl ether. The combined organic layers were washed with brine, dried with $MgSO_4$ and the solvent was removed under reduced pressure. The crude product was purified by column chromatography to give 238 mg (yellow solid, 85%) of compound **6**. ^{1}H NMR (250 MHz, CD_2Cl_2): δ 7.06 (s, 2H), 4.46 (s, 4H), 2.80 (t, J = 7.75 Hz, 4H), 2.58 (t, J = 7.50 Hz, 4H), 1.72−1.53 (m, 8H), 1.27 (br, 72H), 0.90−0.85 (m, 12H). ^{13}C NMR (62.5 MHz, CD_2Cl_2): δ 151.41, 141.18, 139.60, 138.64, 131.27, 130.75, 107.62, 32.44, 32.40, 31.40, 30.16, 30.13, 30.07, 29.99, 29.96, 29.89, 29.83, 28.73, 28.39, 23.15, 14.33. HRMS (ESI+): m/z calcd, 1003.7658; found, 1003.7648.

BDTTQ-1. A suspension of **6** (0.2 mmol), **7** (0.2 mmol) and 15 mL acetic acid were added into a 50 mL Schlenk tube. The mixture were heated to 55 °C and stirred overnight. After cooling down to room temperature, the reaction mixture was filtered, washed with methanol and collected solid, then purified by column using hexane as eluent to get 165 mg of **BDTTQ-1** (green solid, 55%). ^{1}H NMR (250 MHz, $CDCl_3$): δ 8.42 (s, 2H), 7.70 (s, 2H), 2.57 (t, J = 7.50 Hz, 4H), 2.46 (t, J = 7.75 Hz, 4H), 1.55 (br, 8H), 1.27 (br, 72H), 0.88 (br, 12H). ^{13}C NMR (62.5 MHz, $CDCl_3$): δ 150.56, 146.71, 137.50, 136.68, 135.84, 134.42, 134.34, 132.28, 129.33, 119.29, 113.11, 32.15, 31.19, 31.00, 30.43, 30.19, 30.04, 29.95, 29.62, 28.59, 22.89, 14.30. HRMS (ESI+): m/z calcd, 1342.5231; found, 1342.5231.

5,5′-Bis(2-ethylhexyl)-2,2′-bithiophene (9). Bithiophene (**8**) (1.5 g, 9.02 mmol) was dissolved in 40 mL of anhydrous THF. The mixture was cooled down to −78 °C, and a solution of *n*-BuLi (15.75 mL, 25.2 mmol, 1.6 M in hexane) was added. The reaction mixture was stirred for 10 min at this temperature, then a solution of *t*-BuOK (3.83 g, 34.2 mmol in 30 mL THF) was added and kept at −78 °C another 15 min. Afterward, 2-ethylhexyl bromine (3.45 mL, 18.0 mmol) was added in one portion and the mixture was refluxed overnight. The mixture was poured into 100 mL of ice water and hydrolyzed with 1 N HCl, then extracted with diethyl ether (3 × 30 mL). The combined organic phase were dried using Mg_2SO_4, and the solvent was removed under reduced pressure to afford a dark-red oil, which was purified by column chromatography to give 1.51 g (colorless oil, 43%) of compound **9**. ^{1}H NMR (250 MHz, CD_2Cl_2): δ 6.91 (d, J = 3.50 Hz, 2H), 6.65 (d, J = 3.25 Hz, 2H), 2.73 (d, J = 6.50 Hz, 4H), 1.58−1.52 (m, 2H), 1.35 (br, 16H), 0.93−0.87 (br, 12H). ^{13}C NMR (62.5 MHz, CD_2Cl_2): δ 143.79, 135.90, 126.17, 122.87, 41.90, 34.46, 32.80, 29.31, 25.96, 23.46, 14.32, 11.05. HRMS (ESI+): m/z calcd, 391.2493; found, 391.2482.

2,7-Bis(2-ethylhexyl)benzo[1,2-*b*:6,5-*b*′]dithiophene-4,5-dione (10). To a solution of aluminum chloride (768 mg, 5.76 mmol) in 1,2-dichloroethane (25 mL) cooled down to −10 °C was added dropwise a solution of compound **9** (500 mg, 1.28 mmol), pyridine (200 mg, 0.21 mmol) in 1,2-dichloroethane (5 mL) and a solution of oxalyl chloride (0.11 mL, 1.28 mmol) in 1,2-dichloroethane (10 mL). Afterward the mixture was raised to room temperature and stirred overnight. The mixture was poured over ice and extracted with methylene chloride. The extract was washed with water for neutralization and dried over $MgSO_4$. After removing the solvent under reduced pressure, the residue was purified by column chromatography to give **10** as a purple viscous oil (263 mg, 47%).^{1}H NMR (250 MHz, CD_2Cl_2): δ 7.08 (s, 2H), 2.73 (dd, J = 0.75 Hz, J = 6.00 Hz, 4H), 1.64−1.53 (m, 2H), 1.35 (br, 16H), 0.93−0.87 (br, 12H). ^{13}C NMR (62.5 MHz, CD_2Cl_2): δ 175.12, 145.98, 143.14, 135.09, 125.21, 41.70, 34.25, 32.72, 29.23, 25.90, 23.37, 14.27, 10.98. HRMS (ESI+): m/z calcd, 445.2235; found, 445.2246.

4,7-Bis(4-dodecylthiophen-2-yl)benzo[*c*][1,2,5]thiadiazole-5,6-dinitro (12). 4,7-Dibromo-5,6-dinitrobenzodiazole (**4**) (384.0 mg, 1.0 mmol), 2-trimethyltin-4-dodecylthiophene (**11**) (1.04 g, 2.5 mmol), and $Pd(PPh_3)Cl_2$ (70.1 mg, 0.1 mmol) were dissolved in 25 mL of anhydrous THF under argon. The resulting solution was stirred for 16 h at 80 °C. The solvent was removed under reduced pressure to afford a dark-red solid, which was purified by column chromatography to give 0.64 g (light yellow solid, 88%) of compound **12**. ^{1}H NMR (250 MHz, CD_2Cl_2): δ 7.36 (d, J = 1.25 Hz, 2H), 7.34 (d, J = 1.25 Hz, 2H), 2.68 (t, J = 7.25 Hz, 4H), 1.68−1.63 (m, 4H), 1.33−1.27 (m, 36H), 0.90−0.85 (m, 6H). ^{13}C NMR (62.5 MHz, CD_2Cl_2): δ 152.77, 145.11, 142.11, 132.79, 129.76, 126.92, 122.12, 32.49, 30.24, 30.21, 30.15, 29.98, 29.92, 23.25, 14.44. HRMS (ESI+): m/z calcd, 727.3385; found, 727.3362.

4,7-Bis(4-dodecylthiophen-2-yl)benzo[c][1,2,5]thiadiazole-5,6-diamine (13). Compound **12** (0.364 g, 0.5 mmol) and fine iron powder (333 mg, 5.95 mmol) in acetic acid (10 mL) were stirred for 5 h at 75 °C. The reaction mixture was cooled down to room temperature, precipitated in 5% aqueous NaOH and extracted with diethyl ether. The combined organic layers were washed with brine, dried with $MgSO_4$ and the solvent was removed under reduced pressure. The crude product was purified by column chromatography to give 273 mg (yellow solid, 82%) of compound **13**. ^{1}H NMR (250 MHz, CD_2Cl_2): δ 7.19 (d, J = 1.25 Hz, 2H), 7.15 (d, J = 1.25 Hz, 2H), 4.46 (s, 4H), 2.70 (t, J = 7.25 Hz, 4H), 1.73−1.64 (m, 4H), 1.43−1.28 (m, 36H), 0.91−0.85 (m, 6H). ^{13}C NMR (62.5 MHz, CD_2Cl_2): δ 151.45, 144.30, 139.90, 135.60, 130.44, 122.02, 107.62, 32.50, 30.26, 30.22, 30.06, 30.03, 29.93, 23.26, 14.45. HRMS (ESI+): m/z calcd, 667.3902; found, 667.3879.

Compound 14. A suspension of **10** (0.1 g, 0.23 mmol), **13** (0.17 g, 0.25 mmol), and 15 mL of acetic acid were placed into a 50 mL Schlenk tube. The mixture was heated to 55 °C and stirred overnight. After cooling down to room temperature, the product was filtered and washed with methanol and then purified by column using hexane as eluent to give 0.18 g of compound **14** (dark green solid, 73%). ^{1}H NMR (250 MHz, CD_2Cl_2): δ 8.86 (s, 2H), 7.90 (s, 2H), 7.16 (s, 2H), 2.93 (d, J = 6.50 Hz, 4H), 2.73 (t, J = 7.50 Hz, 4H), 1.48 (br, 4H), 1.27 (br, 54H), 1.03−0.88 (br, 18H). ^{13}C NMR (62.5 MHz, CD_2Cl_2): δ 149.92, 143.87, 141.03, 138.38, 136.38, 136.06, 134.02, 133.54, 124.90, 118.56, 118.33, 41.71, 34.58, 33.03, 32.40, 30.27, 30.18, 30.09, 29.97, 29.86, 29.49, 25.95, 23.55, 23.15, 14.49, 14.33, 11.23. HRMS (ESI+): m/z calcd, 1075.5847; found, 1075.5852.

BDTTQ-2. Compound **14** (150 mg, 0.14 mmol) was dissolved in 15 mL of THF at the room temperature. NBS (56.6 mg, 0.32 mmol) was carefully added into the solution in small batches under dark. The mixture was stirred for 5 h. After removing the solvent under reduced pressure, the residue was purified by column chromatography to give **BDTTQ-2** as a dark green solid (146 mg, 78%). ^{1}H NMR (250 MHz, CD_2Cl_2): δ 8.34 (s, 2H), 7.29 (s, 2H), 2.75 (d, J = 6.50 Hz, 4H), 2.35 (t, J = 7.50 Hz, 4H), 1.67−1.59 (br, 4H), 1.48−1.30 (br, 54H), 1.02−0.87 (br, 18H). ^{13}C NMR (62.5 MHz, CD_2Cl_2): δ 149.94, 143.88, 141.04, 138.41, 136.40, 136.10, 134.06, 133.60, 124.95, 118.59, 118.35, 41.76, 34.65, 33.10, 32.44, 30.32, 30.30, 30.28, 30.21, 30.19, 30.00, 29.89, 29.54, 26.01, 23.58, 23.18, 14.51, 14.35, 11.26. HRMS (ESI+): m/z calcd, 1230.3979; found, 1230.4012.

PBDTTQ-1. **BDTTQ-1** (0.1 mmol), compound **15** (0.1 mmol), and chlorobenzene (8 mL) were placed in a 50 mL two-neck flask. The mixture was purged with argon for 5 min, and then 5.5 mg of tris(dibenzylideneacetone)dipalladium(0) ($Pd_2(dba)_3$) and 7.3 mg of tri(*o*-tolyl)phosphine (P(*o*-tolyl)$_3$) were added. Then the mixture was

dx.doi.org/10.1021/ma401938m | *Macromolecules* XXXX, XXX, XXX−XXX

Table 1. Optical and Electrochemical Data of the Polymers

polymer	M_w/M_n[a] (kg/mol)	λ_{abs} (nm) soln[b]	λ_{abs} (nm) film[c]	E_g^{opt} (eV)[c]	E_{HOMO} (eV)[d]	E_{LUMO} (eV)[d]	E_g^{ec} (eV)
PBDTTQ-1	90.7/37.3	358, 422, 860	357, 421, 875	1.18	−5.50	−3.86	1.64
PBDTTQ-2	19.6/11.8	340, 430, 928	340, 438, 978	1.03	−5.48	−4.01	1.47

[a]Determined by GPC in THF using polystyrene standards. [b]Dissolved in choloform ($c = 10^{-5}$ M). [c]Drop-casted from choloform solution (10 mg/mL). [d]HOMO and LUMO levels were estimated from the onsets of the first oxidation and reduction peak, respectively, while the potentials were determined using ferrocene (Fc) as standard by empirical formulas $E_{LUMO} = -(E_{Red}^{onset} - E_{Fc/Fc+}^{1/2} + 4.8)$ eV and $E_{HOMO} = -(E_{Ox}^{onset} - E_{Fc/Fc+}^{1/2} + 4.8)$ eV, wherein $E_{Fc/Fc+}^{1/2} = 0.40$ eV.

heated up to 110 °C under argon. After 3 days, the reaction mixture was poured into methanol. The target polymer was precipitated as olive brown solid and filtered through a Soxhlet thimble, which was then subjected to Soxhlet extraction with methanol, acetone, hexane and chloroform. The polymer was collected from the chloroform fraction and dried in vacuum to afford an olive brown solid (59%). Molecular weight by GPC: M_n = 37.3 K; PDI = 2.43. ^{1}H NMR (250 MHz, CD_2Cl_2): δ 8.96−8.51 (br, 6H), 2.46 (br, 12H), 1.18−0.78 (br, 138H).

PBDTTQ-2. This polymer was prepared from **BDTTQ-2** and **15** in a procedure similar to that for **PBDTTQ-1** as an olive brown solid (63%). Molecular weight by GPC: M_n = 11.8 K; PDI = 1.66. ^{1}H NMR (250 MHz, CD_2Cl_2): δ 9.16−8.10 (br, 6H), 3.0−2.71 (br, 12H), 1.18−0.78 (br, 122H).

RESULTS AND DISCUSSION

Synthesis and Characterization. The synthesis of two monomers is depicted in Scheme 1. Although both monomers have the same skeleton, they were prepared using completely different routes, taking the introduction of solubilizing side chains and bromines at different positions into account. Monomer **BDTTQ-1** was synthesized starting from 2-bromo-3-dodecylthiophene (**1**), which was converted to compound **3** by first introducing *n*-dodecyl via a Grignard reaction then performing stanylation. Stille coupling reaction between **3** and 4,7-dibromo-5,6-dinitrobenzothiadizole **4** produced dinitro compound **5**, which was reduced by iron in acetic acid to obtain diamine **6**. Subsequently, condensation[35] between **6** and diketone **7** gave the monomer **BDTTQ-1**. Monomer **BDTTQ-2** was synthesized using another path from commercial available bithiophene (**8**). Using *t*-BuOK to enhance the reactivity of the lithiated bithiophene was crucially important to obtain diethylhexylbithiophene (**9**).[36] Afterward, diketone **10** was obtained in one step through Friedel−Crafts acylation.[37] Diamine **13** was prepared by two steps in yield of 73%, which was condensed with diketone **10** to give compound **14**. It was then treated with NBS to produce **BDTTQ-2**. The polymerizations were carried out through Stille coupling reaction between **BDTTQ-1** or **BDTTQ-2** and the same donor **15** (Scheme 1).

Both polymers have excellent solubility in chloroform, tetrahydrofuran, toluene, chlorobenzene, etc. The number-average molecular weights (M_n) of the polymers **PBDTTQ-1** and **PBDTTQ-2** were determined as 37.3 and 11.8 K with polydispersity index (PDI) of 2.43 and 1.66, respectively, by GPC method using polystyrene as standard and tetradydrofuran as eluent at room temperature (Table1).

The polymerization was tried several times to enhance the M_n of **PBDTTQ-2**, but the results were similar to those mentioned above. It may arise from the steric hindrance induced by the n-dodecyl in monomer **BDTTQ-2** preventing producing higher molecular weight during polymerization. The thermal properties of the copolymers were investigated by TGA (Supporting Information Figure S1). Both copolymers exhibit excellent thermal stability, with 5% weight loss upon heating at 403 °C, and 422 °C for **PBDTTQ-1** and **PBDTTQ-2**, respectively.

Optical Properties. The optical properties of both polymers were investigated in chloroform solution ($c = 10^{-5}$ M) and in thin films prepared by drop-casting from a 10 mg/mL chloroform solution. The data are summarized in Table 1. In dilute chloroform solution, **PBDTTQ-1** and **PBDTTQ-2** exhibit two main absorption bands as shown in Figure 2a. The

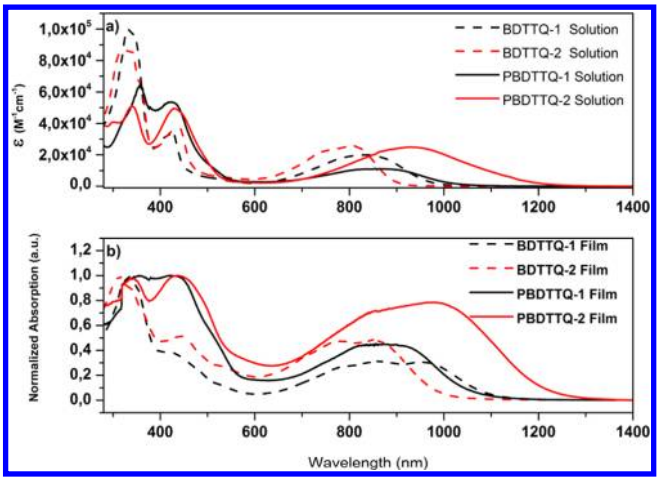

Figure 2. UV−visible−NIR absorption spectra of two monomers and copolymers in (a) chloroform solution ($c = 10^{-5}$ M) and (b) films.

first intense band covers from 300 to 550 nm and the second ranges from 600 to 1200 nm. The higher energy absorption band corresponds to the $\pi-\pi^*$ transition of the conjugated backbone, whereas the lower one should be attributed to intramolecular charge transfer (ICT) between donor and acceptor in the copolymers backbone.[38] To investigate the influence of the different pattern of linkage on the optical properties of the two polymers, the absorptions of two monomers **BDTTQ-1** and **BDTTQ-2** were also recorded and are shown in Figure 2a. Two monomers present $\pi-\pi^*$ transitions at higher energy region and broad absorption band between 600 and 1000 nm similar to those of the corresponding polymers. The latter can be assigned to the ICT from the electron-donating moiety **BDT** to the electron-accepting **TQ** moiety. The difference in maximum absorption of both monomers may originate from the different electron-donating contribution of alkyl chains. Interestingly, compared to the absorption maxima of the monomers, **PBDTTQ-2** exhibits a red shift around 130 nm, while polymer **PBDTTQ-1** shows a smaller red shift of only 40 nm, implying the stronger ICT process in **PBDTTQ-2** than that in **PBDTTQ-1**. This result suggest that electrons are mainly limited on the **TQ** moiety in **PBDTTQ-1**, leading to ineffective charge transfer along the polymer chains, whereas in **PBDTTQ-2**, such a

dx.doi.org/10.1021/ma401938m | *Macromolecules* XXXX, XXX, XXX−XXX

suspension is absent owing to the average distribution of the electron density along the whole polymer backbone. In the film (Figure 2b), the two polymers display slightly broader spectra which are even further bathochromically shifted compared with those in solution. **PBDTTQ-2** shifts to red around 50 nm contrasted with around 15 nm for **PBDTTQ-1**, indicating that **PBDTTQ-2** possesses stronger interaction between the polymer chains than **PBDTTQ-1** in the solid state. The optical band gaps are 1.18 and 1.03 eV, calculated according to the absorption onset of the thin films for **PBDTTQ-1** and **PBDTTQ-2**, respectively. These results demonstrate that the strong acceptor **BDTTQ** is favorable to develop narrow-bandgap copolymers, and the different combination between donor and **BDTTQ** core allow efficient tuning of the optical properties.

Electrochemical Properties. The LUMO and HOMO energy levels of both copolymers were evaluated by cyclic volatammetry (CV) of the thin films. The reduction and oxidation curves of copolymers are shown in Figure 3 and the

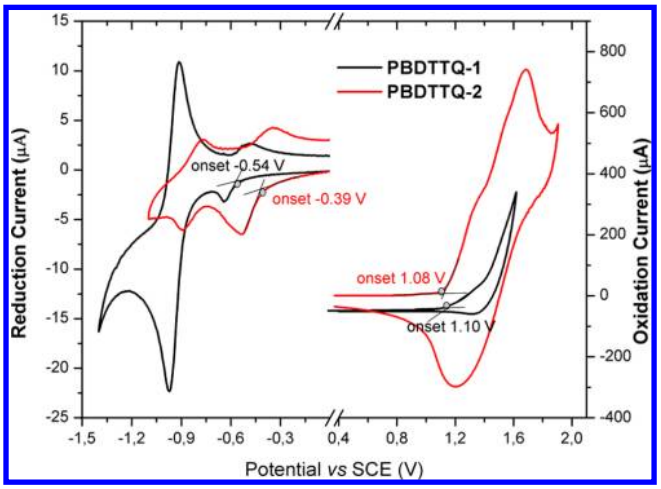

Figure 3. Reduction (left) and oxidation (right) of two polymer films deposited from chloroform.

corresponding electrochemical data are summarized in Table 1. Both copolymers exhibited irreversible oxidation waves and reversible reduction waves, implying their potential in transporting negative charge. On the basis of the onset potentials, the HOMO and LUMO energy levels were estimated to be −5.50 and −3.86 eV for **PBDTTQ-1**, and −5.48 and −4.01 eV for **PBDTTQ-2**, respectively. This result shows that extension of π-conjugation of TQ is a viable strategy to obtain stronger acceptors with lower band gap of the polymers thus possessing deep LUMO and HOMO levels. Moreover, the linkage pattern in **PBDTTQ-2** can obviously lower the LUMO level more than that in **PBDTTQ-1**. The electrochemical band gaps are 1.64 and 1.47 eV for **PBDTTQ-1** and **PBDTTQ-2**, respectively. The difference between the optically and electrochemically measured energy gaps can be explained by the exciton binding energy of the copolymers.[39]

OFET and Self-Organization. The charge carrier transport was studied in field-effect transistors based on a bottom-gate, bottom-contact architecture. The 200 nm thick SiO_2 dielectric was functionalized with hexamethyldisilazane (HMDS) to minimize interfacial trapping sites. The copolymer thin films were deposited by spin-coating 10 mg/mL $CHCl_3$ solution in nitrogen atmosphere, followed by annealing at 150 °C for 1 h. Significant difference in device performance was observed between **PBDTTQ-1** and **PBDTTQ-2**. While **PBDTTQ-1** did not show any field-effect response, **PBDTTQ-2** led to an ambipolar transport with mobilities of 1.2×10^{-3} $cm^2/(V\ s)$ for holes and 6.0×10^{-4} $cm^2/(V\ s)$ for electrons (Figure 4). To

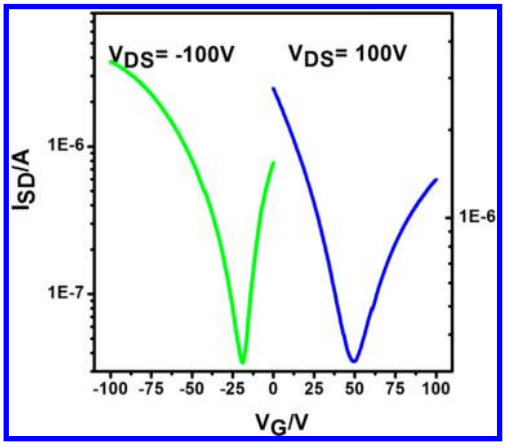

Figure 4. Transfer curves of **PBDTTQ-2** at a source drain bias of V_{SD} = −100 V.

gain an understanding of the device performance, the organization of both copolymers in the bulk and thin film was investigated. For the bulk organization, two-dimensional wide-angle X-ray scattering measurements (2DWAXS) of extruded, macroscopically aligned fibers were performed. For both cases, only equatorial reflections in the small-angle region appeared which were related to the chain-to-chain distance between lamellar stacks aligned along the extrusion direction of the fiber (Figure S2 Supporting Information). A distance of 2.50 nm for **PBDTTQ-1** and 2.20 nm for **PBDTTQ-2** was determined. However, no scattering intensities for the π-stacking were found indicating pronounced disorder of the conjugated polymers in the lamellar structures. The disordered assembly may be due to the high steric hindrance between the alkyl chains as well as the large size of **BDTTQ** unit at the lateral direction not allowing a close and defined packing of the backbones on top of each other. This was further confirmed by the strong amorphous halo of the alkyl side chains. Grazing incidence WAXS (GIWAXS) confirmed the low order also in thin films (Figure S3 Supporting Information). The GIWAXS patterns revealed only one isotropic reflection which was correlated to the chain-to-chain spacing of randomly arranged lamellar structures toward the surface. Therefore, the amorphous morphology should be responsible for the relative low charge mobility. However, no obvious difference was observed for both polymers from the X-ray characterizations which could provide an explanation for the discrepancy between both polymers in device performance. Therefore, density functional theory (DFT) calculations were carried out.

Density Functional Theory Calculation. DFT calculations were carried out on two models of acceptor−donor−acceptor arrangement carrying methyl substituents, named **2T-1** and **2T-2** for **2T-2BDTTQ-1** and **2T-2BDTTQ-2**, respectively. The electron density distributions of the LUMO and HOMO of geometry optimized structures are shown in Figure 5. For both LUMO and HOMO levels of **2T-1**, the electrons are only localized upon one of both electron accepting **BDTTQ** cores, which could prevent the efficient electron transport along the conjugated backbone. This in

dx.doi.org/10.1021/ma401938m | Macromolecules XXXX, XXX, XXX−XXX

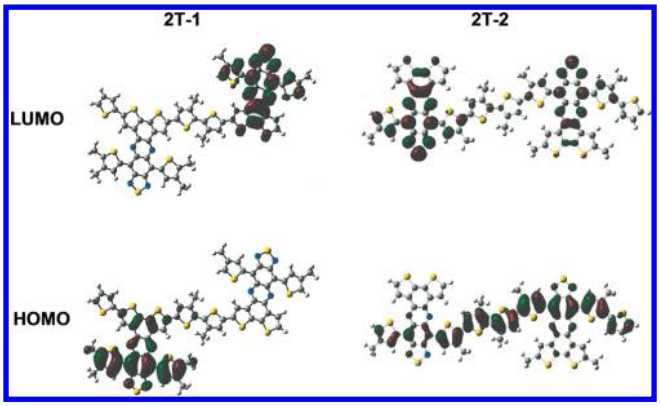

Figure 5. LUMO (top) and HOMO (bottom) distributions for the minimum energy conformations of methyl substituted models of **2T-2BDTTQ-1** (**2T-1**) and **2T-2BDTTQ-2** (**2T-2**) optimized with Gaussian at the B3LYP/6-31G* level.

combination with its disorder assembly prevents interchain charge transfer that produces absent field-effect response for **PBDTTQ-1**. In contrast, electrons of the HOMO and LUMO levels of **2T-2** are both well delocalized over the conjugated repeat unit. This may partly explain the observed ambipolar behavior of **PBDTTQ-2**.[40] In addition, the results from DFT calculations are well consistent with the observations from absorption spectra, demonstrating the stronger ICT process between donor and acceptor in **PBDTTQ-2** than that in **PBDTTQ-1**. It can hence be concluded that the way of linking cannot tune the organization behavior in bulk and in film as verified by the structural analysis but can strongly influence the electron distributions along the polymers chains and therefore the charge carrier mobility.

CONCLUSION

We have successfully synthesized two copolymers **PBDTTQ-1** and **PBDTTQ-2** with different linkage between acceptor **BDTTQ** and donor alkylated bithiophene. With the **TQ** moiety of **BDTTQ** located in the main chains, **PBDTTQ-2** shows narrow optical bandgap of 1.03 eV and relatively low LUMO level of −4.01 eV, approximately 0.15 eV deeper than that for **PBDTTQ-1**, while maintaining deep HOMO level at −5.50 eV. DFT calculations demonstrate that the electronic densities are only localized upon one of both electron accepting **BDTTQ** cores for **2T-1**, whereas the electron density of the LUMO and HOMO are both well delocalized over the conjugated repeat unit for **2T-2**. This is the reason for the pronounced differences of **PBDTTQ-1** and **PBDTTQ-2** in device performance. While **PBDTTQ-1** does not show any field-effect response, **PBDTTQ-2** exhibits an ambipolar transport with mobilities of 1.2×10^{-3} $cm^2/(V\ s)$ for holes and 6.0×10^{-4} $cm^2/(V\ s)$ for electrons. The relatively low mobilities are mainly related to the lack of good π-stacking induced by the alkyl chains, as confirmed by 2DWAXS. It is believed that the charge carrier mobility can be further improved by deliberately reducing the number of alkyl chains in the polymer, on premise of ensuring solubility, to optimize assembled structure of the polymer. The deep LUMO level of **PBDTTQ-2** makes this polymer as potential acceptor for applications in all-polymeric solar cells. This work is currently underway in our laboratory.

ASSOCIATED CONTENT

Supporting Information

TGA, GIWAXS, 2DWAXS, ^{1}H NMR, ^{13}C NMR, and UV−vis plots. This material is available free of charge via the Internet at http://pubs.acs.org.

AUTHOR INFORMATION

Corresponding Author

*(M.B.) E-mail: martin.baumgarten@mpip-mainz.mpg.de.

Present Addresses

†Inst. Materials Res. & Engineering, A Star, 3 Research Link, Singapore 117602.

‡Empa: Swiss Federal Laboratories for Materials Science and Technology, Lerchenfeldstrasse 5, 9014 St. Gallen, Switzerland.

Notes

The authors declare no competing financial interest.

ACKNOWLEDGMENTS

This work is supported by SFB-TR49 and the Max Planck Society (MPG). C.A. gratefully acknowledges the China Scholarship Council (CSC) for offering a scholarship.

REFERENCES

(1) Grimsdale, A. C.; Chan, K. L.; Martin, R. E.; Jokisz, P. G.; Holmes, A. B. *Chem. Rev.* **2009**, *109*, 897−1091.
(2) Günes, S.; Neugebauer, H.; Sariciftci, N. S. *Chem. Rev.* **2007**, *107*, 1324−1338.
(3) Li, C.; Liu, M. Y.; Pschirer, N. G.; Baumgarten, M.; Müllen, K. *Chem. Rev.* **2010**, *110*, 6817−6855.
(4) Arias, A. C.; MacKenzie, J. D.; McCulloch, I.; Rivnay, J.; Salleo, A. *Chem. Rev.* **2010**, *110*, 3−24.
(5) Guo, X.; Baumgarten, M.; Müllen, K. *Prog. Polym. Sci.* **2013**, *38*, 1832−1908.
(6) Yuen, J. D.; Fan, J.; Seifter, J.; Lim, B.; Hufschmid, R.; Heeger, A. J.; Wudl, F. *J. Am. Chem. Soc.* **2011**, *133*, 20799−20807.
(7) Fan, J.; Yuen, J. D.; Wang, M.; Seifter, J.; Seo, J. -H.; Mohebbi, A. R.; Zakhidov, D.; Heeger, A. J.; Wudl, F. *Adv. Mater.* **2012**, *24*, 2186−2190.
(8) Guo, X.; Kim, F. S.; Seger, M. J.; Jenekhe, S. A.; Watson, M. D. *Chem. Mater.* **2012**, *24*, 1434−1442.
(9) Wang, J.; Lu, C.; Mizobe, T.; Ueda, M.; Chen, W.-C.; Higashihara, T. *Macromolecules* **2013**, *46*, 1783−1793.
(10) Bijleveld, J. C.; Zoombelt, A. P.; Mathijssen, S. G. J.; Wienk, M. M.; Turbiez, M.; de Leeuw, D. M.; Janssen, R. A. J. *J. Am. Chem. Soc.* **2009**, *131*, 16616−16617.
(11) Lee, J.; Han, A.-R.; Yu, H.; Shin, T. J.; Yang, C.; Oh, J. H. *J. Am. Chem. Soc.* **2013**, *135*, 9540−9547.
(12) Zhan, X. W.; Tan, Z. A.; Domercq, B.; An, Z. S.; Zhang, X.; Barlow, S.; Li, Y. F.; Zhu, D. B.; Kippelen, B.; Marder, S. R. *J. Am. Chem. Soc.* **2007**, *129*, 7246−7247.
(13) Zhou, E. J.; Cong, J. Z.; Wei, Q. S.; Tajima, K.; Yang, C. H.; Hashimoto, K. *Angew. Chem., Int. Ed.* **2011**, *50*, 2799−2083.
(14) Li, H.; Tam, T. L.; Lam, Y. M.; Mhaisalkar, S. G.; Grimsdale, A. C. *Org. Lett.* **2011**, *13*, 46−49.
(15) Dallos, T.; Hamburger, M.; Baumgarten, M. *Org. Lett.* **2011**, *13*, 1936−1939.
(16) Qian, G.; Qi, J.; Davey, J. A.; Wright, J. S.; Wang, Z. Y. *Chem. Mater.* **2012**, *24*, 2364−2372.
(17) Kitamura, C.; Tanaka, S.; Yamashita, Y. *Chem. Mater.* **1996**, *8*, 570−578.
(18) Tam, T. L.; Li, H.; Lam, Y. M.; Mhaisalkar, S. G.; Grimsdale, A. C. *Org. Lett.* **2011**, *13*, 4612−4615.
(19) Perzon, E.; Zhang, F.; Andersson, M.; Mammo, W.; Inganäs, O.; Andersson, M. R. *Adv. Mater.* **2007**, *19*, 3308−3311.
(20) Lee, Y.; Jo, W. H. *J. Phys. Chem. C* **2012**, *116*, 8379−8386.

(21) Tam, T. L.; Salim, T.; Li, H.; Zhou, F.; Mhaisalkar, S. G.; Su, H.; Lam, Y. M.; Grimsdale, A. C. *J. Mater. Chem.* **2012**, *22*, 18528−18534.
(22) Chen, M. X.; Crispin, X.; Perzon, E.; Andersson, M. R.; Pullerits, T.; Andersson, M.; Inganäs, O.; Berggren, M. *Appl. Phys. Lett.* **2005**, *87*, 252105(1−3).
(23) Cheng, K. F.; Chueh, C. C.; Lin, C. H.; Chen, W. C. *J. Polym. Sci., Part A: Polym. Chem.* **2008**, *46*, 6305−6316.
(24) Zhang, X.; Steckler, T. T.; Dasari, R. R.; Ohira, S.; Potscavage, W. J.; Tiwari, S. P.; Coppée, S.; Ellinger, S.; Barlow, S.; Brédas, J. L.; Kippelen, B.; Reynolds, J. R.; Marder, S. R. *J. Mater. Chem.* **2010**, *20*, 123−134.
(25) Dallos, T.; Beckmann, D.; Brunklaus, G.; Baumgarten, M. *J. Am. Chem. Soc.* **2011**, *133*, 13898−13901.
(26) Qian, G.; Zhong, Z.; Luo, M.; Yu, D.; Zhang, Z.; Ma, D.; Wang, Z. Y. *J. Phys. Chem. C* **2009**, *113*, 1589−1595.
(27) Frisch, M. J. et al. *Gaussian 03, Revision B.04*; Gaussian, Inc.: Pittsburgh PA, 2003.
(28) Becke, A. D. *J. Chem. Phys.* **1993**, *98*, 1372−1377.
(29) Lee, C. T.; Yang, W. T.; Parr, R. G. *Phys. Rev. B* **1988**, *37*, 785−789.
(30) Usta, H.; Risko, C.; Wang, Z. M.; Huang, H.; Deliomeroglu, M. K.; Zhukhovitskiy, A.; Facchetti, A.; Marks, T. J. *J. Am. Chem. Soc.* **2009**, *131*, 5586−5608.
(31) Wang, E. R.; Hou, L. T.; Wang, Z. Q.; Hellström, S.; Mammo, W.; Zhang, F. L.; Inganäs, O.; Andersson, M. R. *Org. Lett.* **2010**, *12*, 4470−4473.
(32) Meyer, A.; Sigmund, E.; Luppertz, F.; Schnakenburg, G.; Gadaczek, I.; Bredow, T.; Jester, S. S.; Höger, S. *Beilstein J. Org. Chem.* **2010**, *6*, 1180−1187.
(33) Biniek, L.; Fall, S.; Chochos, C.; Anokhin, D. V.; Ivanov, D. A.; Leclerc, N.; Lévêque, P.; Heiser, T. *Macromolecules* **2010**, *43*, 9779−9786.
(34) Yue, W.; Zhao, Y.; Tian, H. K.; Song, D.; Xie, Z. Y.; Yan, D. H.; Geng, Y. H.; Wang, F. S. *Macromolecules* **2009**, *42*, 6510−6518.
(35) Tsubata, Y.; Suzuki, T.; Yamashita, Y.; Mukai, T.; Miyashi, T. *Heterocycles* **1992**, *33*, 337−348.
(36) Leroy, J.; Levin, J.; Sergeyev, S.; Geerts, Y. *Chem. Lett.* **2006**, *35*, 166−167.
(37) Belen'kii, L. I.; Shirinian, V. Z.; Gromova, G. P.; Kolotaev, A. V.; Strelenko, Y. A.; Tandura, S. N.; Shumskii, A. N.; Krayushkin, M. M. *Khim. Geterotsikl. Soed.* **2003**, *12*, 1785−1793.
(38) Kim, B.; Yeom, H. R.; Yun, M. H.; Kim, J. Y.; Yang, C. *Macromolecules* **2012**, *45*, 8658−8664.
(39) Sariciftci, N. S. *Primary Photoexcitations in Conjugated Polymers: Molecular Excitions vs Semiconductor Band Model*; World Scientific: Singapore, 1997.
(40) Ashraf, R. S.; Kronemeijer, A. J.; James, D. I.; Sirringhaus, H.; McCulloch, I. *Chem. Commun.* **2012**, *48*, 3939−3941.